minerals

MDPI

Article

Thermal Stability of Calcium Oxalates from CO_2 Sequestration for Storage Purposes: An *In-Situ* HT-XRPD and TGA Combined Study

Nadia Curetti [1], Linda Pastero [1,*], Davide Bernasconi [1], Andrea Cotellucci [1], Ingrid Corazzari [2], Maurizio Archetti [3] and Alessandro Pavese [1]

[1] Earth Sciences Department, Università Degli Studi di Torino, 10125 Torino, Italy; nadia.curetti@unito.it (N.C.); davide.bernasconi@unito.it (D.B.); andrea.cotellucci@unito.it (A.C.); alessandro.pavese@unito.it (A.P.)
[2] Chemistry Department, Università Degli Studi di Torino, 10125 Torino, Italy; ingrid.corazzari@unito.it
[3] EcoSpray Technologies S.r.l., 15050 Alzano Scrivia, Italy; archetti@ecospray.eu
* Correspondence: linda.pastero@unito.it

Abstract: Calcium oxalates are naturally occurring biominerals and can be found as a byproduct of some industrial processes. Recently, a new and green method for carbon capture and sequestration in stable calcium oxalate from oxalic acid produced by carbon dioxide reduction was proposed. The reaction resulted in high-quality weddellite crystals. Assessing the stability of these weddellite crystals is crucial to forecast their reuse as solid-state reservoir of pure CO_2 and CaO in a circular economy perspective or, eventually, their disposal. The thermal decomposition of weddellite obtained from the new method of carbon capture and storage was studied by coupling *in-situ* high-temperature X-ray powder diffraction and thermogravimetric analysis, in order to evaluate the dehydration, decarbonation, and the possible production of unwanted volatile species during heating. At low temperature (119–255 °C), structural water release was superimposed to an early CO_2 feeble evolution, resulting in a water-carbon dioxide mixture that should be separated for reuse. Furthermore, the storage temperature limit must be considered bearing in mind this CO_2 release low-temperature event. In the range 390–550 °C, a two-component mixture of carbon monoxide and dioxide is evolved, requiring oxidation of the former or gas separation to reuse pure gases. Finally, the last decarbonation reaction produced pure CO_2 starting from 550 °C.

Keywords: weddellite; dehydration; decarbonation; thermal decomposition; HT-XRPD; TGA-FTIR

Citation: Curetti, N.; Pastero, L.; Bernasconi, D.; Cotellucci, A.; Corazzari, I.; Archetti, M.; Pavese, A. Thermal Stability of Calcium Oxalates from CO_2 Sequestration for Storage Purposes: An *In-Situ* HT-XRPD and TGA Combined Study. *Minerals* **2022**, *12*, 53. https://doi.org/10.3390/min12010053

Academic Editors: Ting Xiao, Hailong Tian and Jize Piao

Received: 22 November 2021
Accepted: 28 December 2021
Published: 30 December 2021

1. Introduction

Calcium oxalate ($CaC_2O_4 \cdot xH_2O$) at various hydration degrees is a naturally occurring biomineral found in fossils, plants, human urinary stones, and a byproduct of some industrial processes, such as those involving paper, food, and beverage production. Due to its importance in the biomedical field and cultural heritage preservation, calcium oxalate stability has been extensively investigated, mainly using thermogravimetric analysis, infrared, and Raman spectroscopies [1–8].

Calcium oxalate crystallizes in three hydrated forms: the monoclinic monohydrate (COM, $CaC_2O_4 \cdot H_2O$; whewellite), the tetragonal dihydrate (COD, $CaC_2O_4 \cdot (2 + x)\ H_2O$, $x < 0.5$; weddellite), and the triclinic trihydrate (COT, $CaC_2O_4 \cdot xH_2O$, $2.5 < x < 3.0$; caoxite). In addition, the anhydrous phase (COA) is obtained by dehydration of the former. Monohydrate thermal stability has been accurately studied along with the anhydrous phase.

Our previous papers [9,10] proposed a CO_2 capture/storage reaction, in which the ascorbic acid aqueous solution is used as a reducing agent of carbon dioxide to form oxalic acid. In the presence of calcium as the counterion, weddellite (COD) precipitates. The quality of weddellite crystals was investigated at room conditions by X-ray single-crystal diffraction experiments. COD samples exhibited a very high crystal quality, differing from

each other only for the zeolitic water content, reflecting different precipitation paths as a function of the experimental setups.

The thermal behavior of weddellite crystals is crucial in assessing their carbon dioxide storage capacity, disposal, or, eventually, reuse in a circular economy perspective. COD could be considered a solid-state carbon dioxide reservoir, reducing storage and handling safety costs compared to compressed gas. Calcium oxalate can be a potential source of pure CO_2 and CaO, exploiting thermal degradation. CO_2 recovered from calcium oxalate may be used in standard applications, while homogeneous [11–14] calcium oxide powder can be employed as a reagent in the cement or ceramics industries.

Nevertheless, the literature reports a comparatively modest number of studies regarding the decomposition of oxalates using *in-situ* X-ray powder diffraction (XRPD), which is appropriate to provide a complete description and quantification of the crystalline phases appearing at different stages of the reaction.

In this framework, the present study combines *in-situ* XRPD and thermal-gravimetric analysis (TGA) to explore the thermal evolution of COD crystals from carbon capture (setup B, Figure S1 in the Supplementary Materials), and the products of the thermal degradation. XRPD and TGA experiments were performed under an oxidant atmosphere and by applying heating conditions close to a large-scale treatment oven, where the use of a conditioned atmosphere would be economically unfavorable. The thermal degradation pathways explored by XRPD and TGA were compared, notwithstanding setup differences and unequal heat transfer rates.

1.1. Decomposition Pathways

Thermal degradation reactions of calcium oxalate (monohydrate) have been reported by several authors due to the interest in calcium oxalate as a standard for TGA calibration [1,4,15–21]:

The first step (dehydration) represents an endothermic process both in the inert and oxidizing atmosphere, according to the reactions R1:

$$CaC_2O_4 \cdot H_2O \leftrightarrow CaC_2O_4 + H_2O \text{ (reaction R1).}$$

$$CaC_2O_4 \rightarrow CaCO_3 + CO \text{ (reaction R2a)}$$

$$CaCO_3 \leftrightarrow CaO + CO_2 \text{ (reaction R3)}$$

R2a is an endothermic reaction under inert conditions, but possibly exothermic in air or oxygen, and R3 is endothermic.

Additional reactions may occur in the reaction batch, simultaneously with R2a: disproportionation (R2b) and oxidation (R2c and R2d).

The disproportionation has been proposed [8,15,17–19,22] to explain the presence of both CO and CO_2 in the reaction batch:

$$2CO \rightarrow C + CO_2 \text{ (reaction R2b)}$$

The disproportionation reaction is considered a very slow process and neglected in many works dealing with calcium oxalate thermal decomposition [16,17,19,23]. CO, in turn, may coexist with CO_2 in the carbonate formation range of temperature.

The oxidation of CO to CO_2 may be related to the catalytic effect of some parts of the experimental setup (the platinum crucible, for instance [1,19,23–25]):

$$CO + 1/2O_2 \rightarrow CO_2 \text{ (reaction R2c)}$$

The occurrence of free carbon is considered a side-effect typical of the decomposition of REE-oxalates [1], or as a ubiquitous byproduct, even in calcium oxalate decomposition [17,19,23].

$$C + O_2 \rightarrow CO_2 \text{ (reaction R2d)}$$

1.2. Previous Kinetic Investigations

The kinetics of reactions R1, R2a, and R3 have been studied using thermogravimetric techniques working in static air atmosphere, vacuum, or sweeping gas fluxes both in an inert atmosphere and in air [1–4,17,26].

The kinetics of thermal degradation for reactions R1 and R3 strongly depend on the experimental conditions due to the reversibility of dehydration and decarbonation, whereas R2a is irreversible [1,17,18]. Moreover, heat and mass counter-compensate their common variations, changing the decomposition temperatures and demonstrating the dependence of the degradation reactions on the transport mechanisms [18].

The temperatures related to the maximum reaction rate (reactions R1, R2a, and R3) roughly range from 45 to 235 °C, from 250 to 550 °C, and from 550 to 850 °C, respectively, and depend on experimental aspects, such as the preparative routine, the environmental conditions, the heating rate, the presence and nature of the flowing gas, as well as the hydration state of the crystalline phase (COT, COD or COM) [2,4,8,16,18–20]. Furthermore, heat and mass transfer in thermal analysis seriously affect the kinetics of the reactions and have become even more crucial for fast heating experiments. Low mass and slow heating rate experiments are generally considered free from artifacts due to heat and mass transfer [27,28], although this statement is not always fully satisfied [18].

It has been demonstrated that the temperature of the maximum reaction rate increases according to the sequence flowing air/static air/flowing nitrogen [15]. Dehydration is moderately affected by the nature of the atmosphere surrounding the sample.

TGA data analysis [4,16–19] or quantum chemical prediction [5] allow the determination of the activation energies of the processes involved in the thermal degradation of calcium oxalate. As with reaction temperatures, activation energies are strongly dependent on the size and shape of the crucible, heat and mass transfer (gas fluxes or vacuum), and the presence of some carbon as a byproduct, exerting a catalytic effect on the CO to CO_2 transformation. Lapidary, in 1980, Price et al. [19] declared that "the selection of CaC_2O_4 as a "model" compound to show the applicability of a particular method of analyzing the kinetic data obtained in the vacuum cannot be justified", questioning the activation energy resulting from thermogravimetric methods.

Almost all of the papers devoted to determining the thermal stability of oxalate are referred to as calcium oxalate monohydrate. Whewellite shows higher structural order than weddellite that contains loosely bonded zeolitic water molecules free to move in the channels [7]. Accordingly, the transition temperatures are significantly higher for whewellite. The dehydration reaction of weddellite occurs at lower temperatures than whewellite, confirming the hypothesis of weakly bonded water molecules in the channels of weddellite [7,16,29]. Fourier transform infrared spectroscopy (FTIR) experiments by Conti et al. [6] at low temperatures (95 and 173 K) confirmed the different structural ordering of the two crystal phases and the presence of disordered zeolitic water in weddellite crystals, which results in the lower temperature of dehydration.

Furthermore, the relative storage humidity plays an essential role in the stability of weddellite crystals. It has been demonstrated that the transformation of whewellite in weddellite takes a few minutes when original whewellite crystals are immersed in water. As the humidity decreases, the time required to reach the stability increases [6]. Nevertheless, this is of primary importance when considering the storage of calcium oxalates produced by carbon dioxide reduction.

Coupled TGA and XRPD experiments have been proposed by Izatulina et al. [30,31]. They investigated the thermal stability of natural (from renal stones) and synthetic COM in the "low" (−173 to +170 °C) and "high" (+25 to +150 °C) temperature ranges by *in situ* XRPD experiments. A first transition to α-COA at 130° was observed. At 150 °C, the COM phase completely disappeared. A further transformation from α to β-COA starts at 310 °C and achieves completion at 340 °C. In agreement, from experiments [16,32] and quantum mechanical calculations, Zhao [33] proposed four polymorphs of COA.

One additional transition from low temperature to high temperature whewellite was recognized between 55 and 75 °C [22,30]. Weddellite resulted in stable recordings of up to 140 °C. The transition from COD to COA occurs at a temperature of 150 °C, while the appearance of the COM phase is reported only after three heating cycles [7]. The COA polymorph observed here matches the fourth polymorph by Zhao [33]. As with COM, COD decomposes in three stages: 23–60 °C (decrease of the parameter *a* and of the cell volume), 70–105 °C (a slight increase of the parameter *c* due to the mechanical compression of the channels, and as a result of the zeolitic water release and almost isotropic thermal expansion), and 110–126 °C (the cell parameters plummet due to the general rearrangement of the structure, and as a result of the release of the framework water molecules), followed at 130 °C by the dehydration and transition to the α-COA phase that could be considered complete at 150 °C.

While the transformation of whewellite at room temperature and pressure is a reversible process leading to (and back from) α-COA, the transformation of COD is less straightforward and gives the monohydrate phase both at HT and RT. The reaction kinetics at room temperature are slow. At HT, the conversion into the monohydrate phase occurs at 140 and 150 °C, with complete conversion of COD into the α-COA phase.

Thermal degradation of calcium oxalate has been assessed by the *in-situ* environmental SEM analysis, as well [20]: the crystal morphology is preserved during reactions R1 and R2a, while after reaction R3, crystals are substituted by calcium oxide pseudomorphic on calcium oxalate, giving evidence of a recrystallization process.

2. Materials and Methods

Calcium oxalate dihydrate (weddellite) was precipitated from CO_2 by carbon reduction using a Ca-ascorbate aqueous solution exploiting the reaction described elsewhere [9,10]. The suspension was vacuum filtered on a cellulose filter with a pore size of 0.45 μm. After filtering, the crystalline sample was dried overnight at room temperature.

The subsequent experiments were conducted in non-equilibrium conditions.

2.1. In-Situ XRPD Experiments

In-situ high-temperature (HT) XRPD data collections at quasi-equilibrium/equilibrium (data collections at given *T* after the achievement of thermal equilibrium as reported in the Supplementary Materials, Table S1) were carried out using a Rigaku SmartLab XE (Rigaku, Tokyo, Japan) diffractometer (Bragg-Brentano θ-θ geometry, CuKα radiation, generator operating at 40 kV and 30 mA) equipped with a Rigaku Multipurpose High Temperature Attachment, combined with PTC-EVO temperature control. The actual temperature of the sample was determined using a calibration curve previously defined.

The samples were heated at a rate of 15 °C/min (Table S1; Supplementary Materials), in keeping with the heating ramp proposed by Hourlier [17] and summarized in Table S2, and held at the achieved temperature for 30 min. Diffraction patterns were recorded using a CCD detector (Rigaku Hypix 3000), operating as a punctual detector in the range $5 < 2\theta < 80°$ with a speed of 1°/min and step size of 0.01°. The heating rate was maintained constant throughout the XRPD experiments to prevent temperature shifts related to the heat transfer. The temperatures at which XRPD data were collected are reported in Table S1 (Ramp#1, Supplementary Materials). Ramp#1 did not allow complete characterization of the recrystallization reactions. Two more runs (Ramp#2 and Ramp#3) were designed and carried out to complement and detail Ramp#1.

Phase identification from XRPD data was performed using the DIFFRAC.EVA software (version 11.0.0.3, Bruker Corporation, Ettlingen, Germany) and the PDF-2 database. The GSAS-II Software Package (Argonne National Laboratory, UChicago Argonne LLC, Lemont, IL, USA) was used for full profile refinements to quantify and characterize the crystal phases occurring in the mixture that develops from the transformations of Ca-oxalate.

2.2. Thermogravimetric Analysis-Evolved Gas Analysis (TGA-EGA)

Thermogravimetric analysis coupled with infrared spectrometry (TGA-FTIR) was used to assess the COD thermal behavior and monitor the species evolved during the thermal degradation (CO, CO_2, and H_2O). In detail, the TGA-FTIR setup was previously cleaned by purging nitrogen and raising the temperature until 930 °C to remove any pollutant from the measure system. After the cleaning cycle, the sample (6.27 mg) was placed in a platinum pan and put in a Pyris 1 thermobalance (Perkin Elmer, Waltham, MA, USA). Then, the sample chamber was sealed at room pressure and gas purged at 35 mL/min for 30 min with an oxygen-nitrogen mixture (33.3% of O_2 in N_2). Thereafter, the sample was heated under flowing of the same oxidant gas mixture from 70 to 900 °C at different heating rates depending on the temperature range: between 72 to 250 °C, a slow heating rate (2 °C/min) was chosen to better discriminate zeolitic and structural water. At a higher temperature (250 to 900 °C), the sample was heated at 15 °C/min to identify the nature and monitor the evolution of the gaseous species that evolved during the formation of solid phases other than hydrated oxalates investigated by XRPD experiments.

The gas that evolved during the heating ramp was piped (gas flow 65 mL/min) via a pressurized transfer line (Redshift S.r.l., San Giorgio in Bosco (PD), Italy) and analyzed continuously by FTIR spectrophotometer (Spectrum 100, Perkin Elmer), equipped with a thermostatic conventional gas-flow cell. Temperature/time-resolved spectra were acquired in the 4000–600 cm^{-1} wavenumber range and analyzed with the Spectrum software (version 10, Perkin Elmer, Waltham, MA, USA).

Temperature-resolved infrared profiles of the evolved gases were obtained from the absorbance variation at a specific wavenumber characteristic of each gaseous species of interest (1650, 2185, and 2359 cm^{-1} for H_2O, CO, and CO_2, respectively).

The deconvolution of the FTIR and derivative thermogravimetry (DTG) curves was performed using the Fityk 0.9.8 free software (Marcin Wojdyr, Institute of High Pressure Physics, Warsaw, Poland, [34]) and choosing a Voigt or a splitted Voigt (for strong peak asymmetry) peak profile to fit the experimental data.

3. Results

Figure 1 shows the results of *in-situ* HT-XRPD experiments, heating weddellite according to Ramp#1, to investigate the correlation between solid-state phases stable within a temperature range and gases evolving from thermal degradation of calcium oxalate.

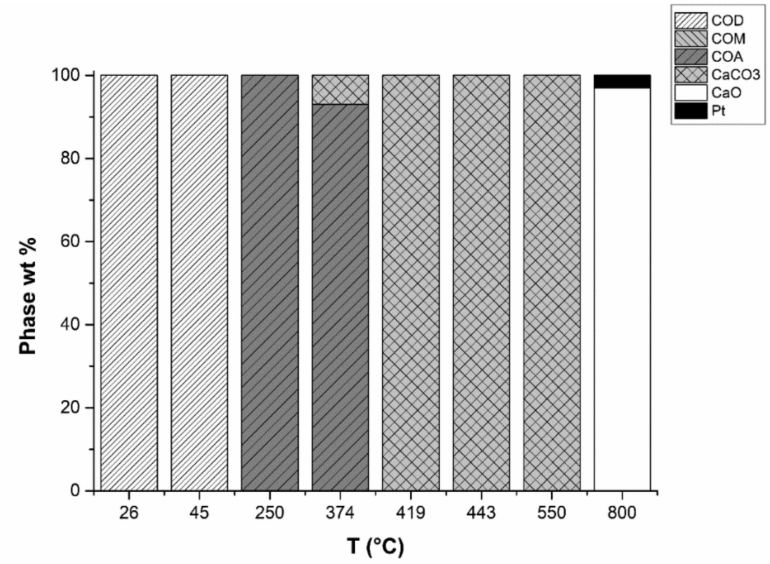

Figure 1. Ramp#1: The transitions between crystal phases are not well distinguished. Weddellite to whewellite transition is missing, as the anhydrous phase abruptly appears at 250 °C. The same applies for CaO, which suddenly crystallizes at 800 °C. Pt signal comes from the sample holder.

During the first two steps (26 and 45 °C), calcium oxalate dihydrate is the stable phase. The transition from COD to COA occurs between 45 and 250 °C and a COM fraction is not recorded. At 250 °C, weddellite is fully dehydrated, with COA identified as the sole crystalline phase. At 374 °C, some calcium carbonate (calcite) appears and at 419 °C it completely replaces COA. Calcium carbonate, in turn, is stable until the last-but-one step, at 550 °C, where the onset of the decarbonation reaction is detected. Calcium carbonate lasts up to 800 °C. Starting from this temperature only CaO occurs (Pt diffraction signal comes from the powder sample holder).

Ramp#2 represents an intermediate experiment intended to find the proper measurement conditions in terms of temperature. Details regarding Ramp#2 (actual temperature and related stable crystal phases) are given in Table S1 and Figure S2 of the Supplementary Materials. Eventually, Ramp#3 (Figures 2 and 3) was designed to detail the crystalline phase transitions.

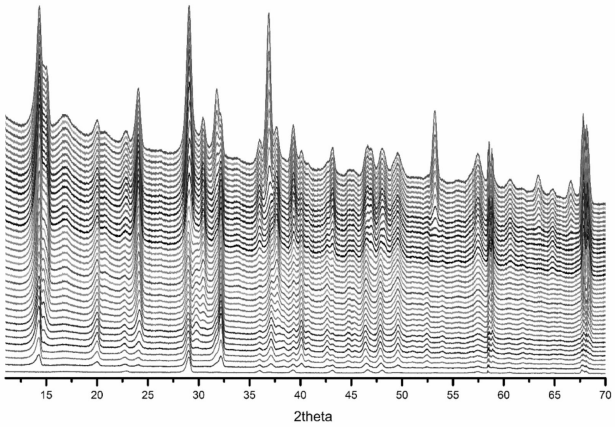

Figure 2. Raw data of HT-XRPD *in-situ* measurement (Ramp#3).

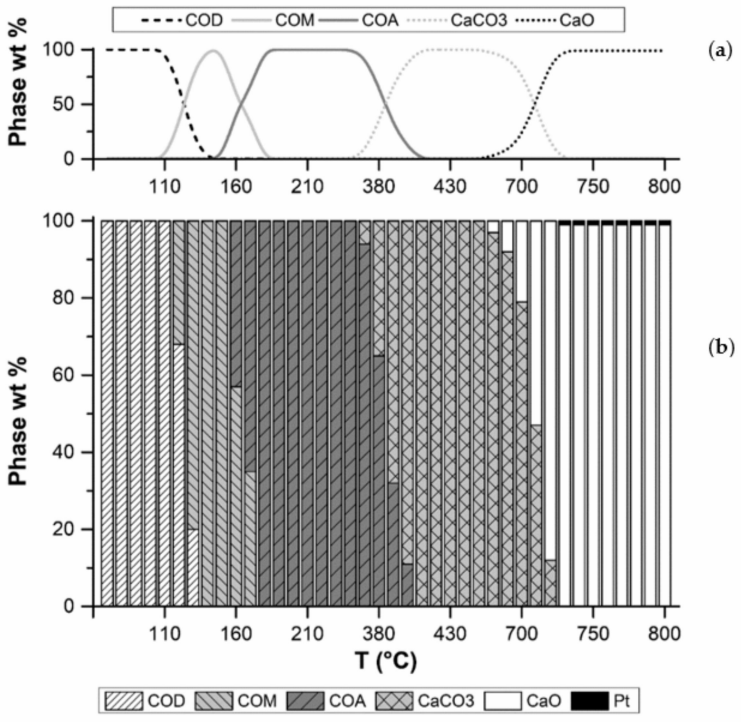

Figure 3. Ramp#3. The HT-XRPD refinement and quantitative analysis highlight the thermal stability range of the phases coming from COD thermal degradation (**a**) and the transition between crystalline phases (**b**).

The first transition between weddellite and whewellite approximately starts at 110 °C and achieves completion at 140 °C (Figure 3). During this first transition, the weight loss recorded by TGA analysis is related to zeolitic water. Between 140 and 150 °C, in a very narrow T-range, the sole stable phase is the calcium oxalate monohydrate that undergoes further dehydration between 150 and 180 °C, losing the tightly bonded structural water. COA is stable up to 410 °C. The onset of the decarbonation reaction is detectable from 360 °C. In the range 410–680 °C, calcium carbonate is the unique stable phase, but at higher temperatures, it is progressively replaced by CaO. At the end of the reaction (800 °C), the final crystalline product is fine-grained pure lime, reusable in classical applications, such as cement or ceramics.

Of note, in any explored ramp, the Pt signal from the sample holder becomes visible due to the volume loss of the sample.

The quantitative analysis of the XRPD data was complemented with the unit cell volume evaluation for each crystalline phase formed. Data calculated are reported in Figure S3. As expected, some thermal drift can be observed, but the overall values are constant for each crystalline phase.

The thermal decomposition of the sample was monitored in the temperature range between 70 and 900 °C (2 °C/min up to 250 °C and 15 °C/min from 250 to 900 °C) and shows three weight loss processes, as illustrated in Figure 4.

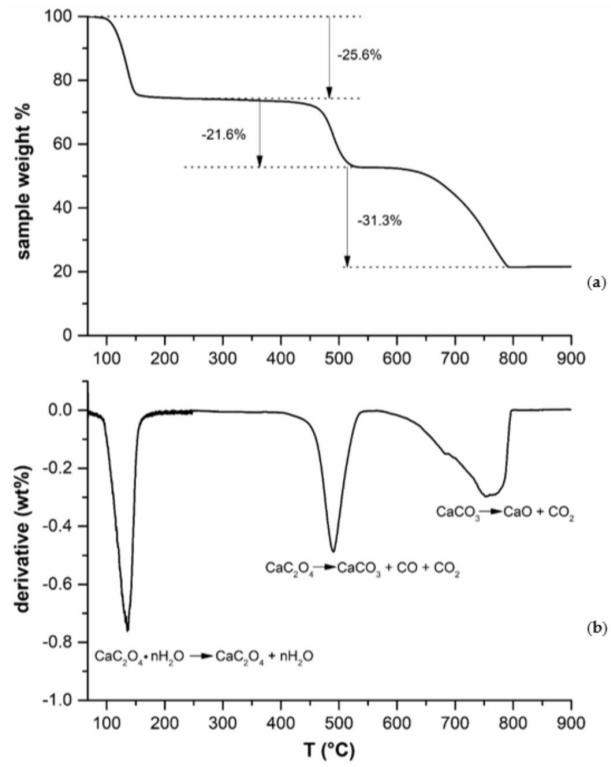

Figure 4. Thermogram (**a**) and the first derivative (**b**) showing the endothermic peaks related to the reactions indicated in correspondence.

The first process, which occurs between 70 and 200 °C (maximum rate at 136 °C), corresponds to a weight loss of 25.6% and is related to the evolution of both zeolitic and structural water. Ideally, the water lost during heating should represent 22% of the weight of the sample. Data from FTIR measurements (Figure 5a–c) confirm that CO_2 is evolved during heating (Figure 5c), even at low temperatures (119–255 °C), justifying the difference in weight loss. This faint evolution of CO_2 in the low-temperature range perfectly overlaps H_2O evolution and possibly represents the onset of the structural collapse of weddellite at low temperature (150 °C). This is possibly related to the stabilization of α-COA, as reported by Izatulina [30,31] and Zhao [33], even if from the XRPD analysis, no COA,

calcium carbonate or lime were detected in this temperature range, probably due to values below the detection limits. Therefore, this lower value must be cautiously considered the temperature limit for weddellite stability for storage purposes.

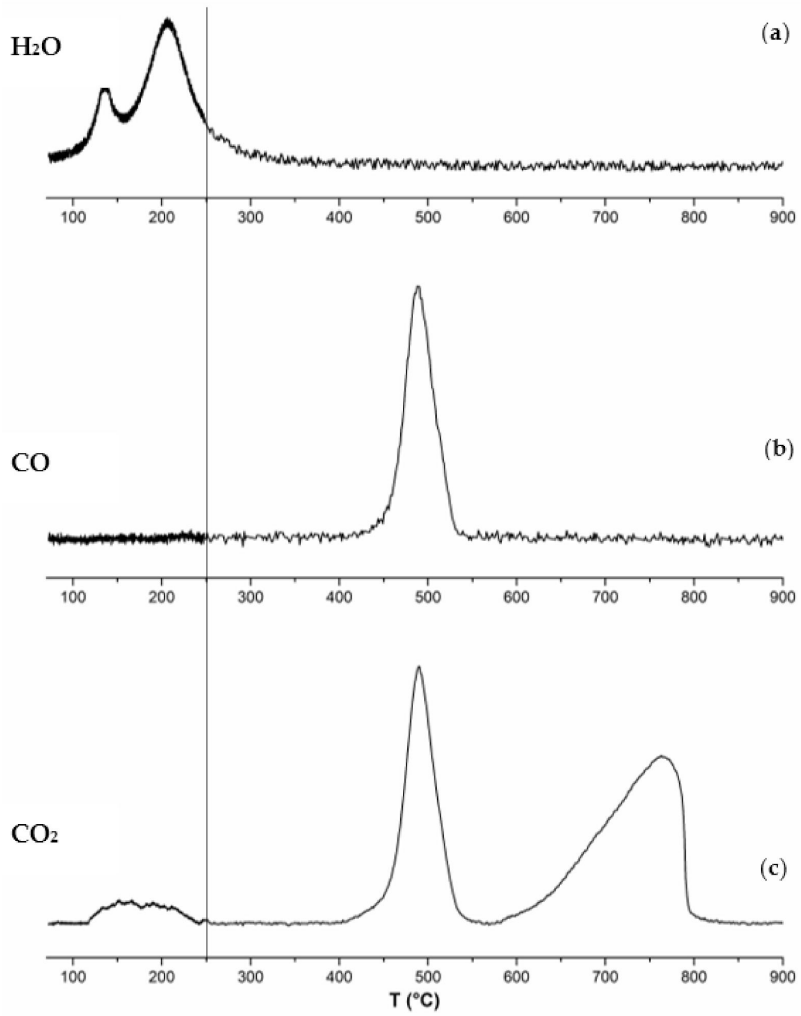

Figure 5. FTIR measurements of (**a**) H_2O, (**b**) CO, and (**c**) CO_2 release. The darker color of the experimental data on the left of the vertical line (low-temperature range) is related to the slow-rate ramp (2 °C/min), at a temperature higher than 250 °C, the ramp rate was increased to 15 °C/min to simulate the heating condition of an industrial oven.

The two water release curves can be roughly recognized: the first, with a maximum at 152.8 °C; the second, with a maximum at 200.9 °C from FTIR data. This agrees with the literature [17]. The FTIR profile of H_2O release (Figure 5a) shows a double peak in the temperature range of 70—300 °C. The first maximum is at 135 °C, the second one at 206.6 °C (for the decomposition of the FTIR curves, please refer to the Supplementary Materials section, Figure S4). The two maxima correspond to the evolution of the zeolitic and structural water. In terms of solid phases, they correspond to the dehydration steps of the oxalate, from COD to COM and then to COA. The release of H_2O from the crystal structure continues up to approximately 300 °C. Structural H_2O and the second CO_2 evolution occur at almost the same temperature, indicating that calcium oxalate sets up to collapse at a lower temperature than expected (during the massive loss of carbon monoxide and dioxide reported in the literature), approximately at 150 °C.

The second weight-loss (21.6%) occurs in the range 390–550 °C, with a maximum value at 490 °C. During this step, both CO and CO_2 (Figure 5b,c) are released according to the literature [1,17,21]. In agreement with the stoichiometric calculation, CO would lead to

a weight loss of 17%, the difference with the actual is attributed to some CO_2 that evolved during the heating, as confirmed by FTIR measurements (Figure 5b). The maximum release temperature for CO_2 and CO are at 492.6 and 488.1 °C, respectively.

A third remarkable weight loss (31.3% b) occurs between 550 and 800 °C. A split-Voigt function was used to simulate the asymmetry of experimental peaks. The maximum release of CO_2 occurs at a temperature of about 767 °C. Immediately beyond the maximum release temperature, CO_2 drops, indicating the completion of the degradation reactions of calcium oxalate, in full agreement with diffraction data. According to the literature, the CO_2 release may account for a weight loss of 27%. The difference is attributed to a partial superimposition of the second and third steps due to the relatively high heating rate.

This last decomposition reaction kinetics is clearly affected by the comparatively slow removal of gases due to oxalate decomposition from the HT-chamber. The asymmetric peak related to the evolved CO_2 develops slowly compared to the previous decomposition steps. The asymmetry could reflect a forward-backward reaction due to the reaction chamber's high CO_2 and calcium oxide substrate activities, related to lingering volatile species (Topley-Smith effect). It is worth recalling that the heat and mass flow compensate for mutual fluctuations.

In Figure 6 and the related Table S3 of Supplementary Materials, the temperatures related to the three degradation reactions of weddellite revealed by XRPD (appearance and disappearance of the crystalline phases) and DTG (gas evolution) are summarized and compared. The transition temperature ranges agree with those from the literature [7,17].

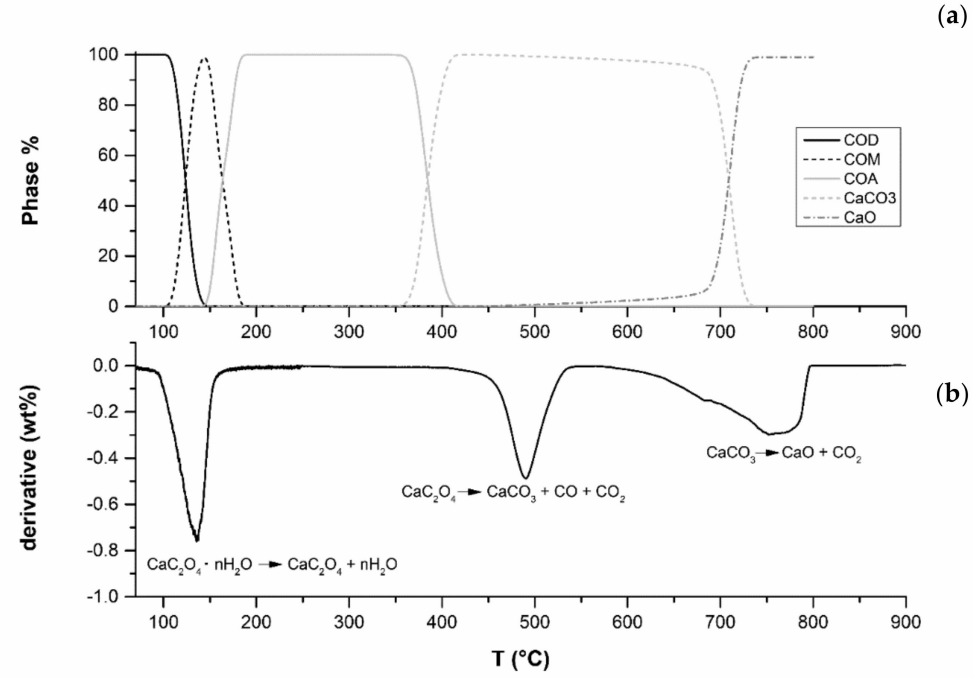

Figure 6. XRPD (**a**) data related to the appearance/disappearance of crystal phases from the decomposition of weddellite compared with the DTG (**b**) calculated from TG data.

HT-XRPD and TGA experiments provide coherent descriptions of zeolitic and structural water release. The DTG peak related to water release overlaps the temperature range of the transition COD → COM → COA, not providing an accurate characterization via thermal-gravimetric analysis. We stress that, in TGA, a 2 °C/min ramp was chosen to emphasize the double water loss. In contrast, in HT-XRPD, we recorded patterns at narrow temperature intervals to follow the transformation of the solid phases from weddellite to whewellite and then to the anhydrous phases. Although a general shift to higher temperature occurs owing to heat and mass transfer related effects, the releases of volatile phases can be undoubtedly associated with the stabilization of the crystalline phases recorded by XRPD, following the sequence:

$$CaC_2O_4 \cdot xH_2O \leftrightarrow CaC_2O_4 + xH_2O \text{ (reaction R1)}$$

where x is equal to 2 (weddellite to whewellite; zeolitic water loss) or 1 (whewellite to anhydrous Ca-oxalate; structural water loss);

$$CaC_2O_4 \rightarrow CaCO_3 + CO + CO_2 \text{ reaction R2a (and reactions R2b, R2c, and R2d)}$$

corresponding to the transition from anhydrous Ca-oxalate to calcite (first decarbonation reaction), accompanied by carbon monoxide and dioxide release and not, as suggested in some literature [1,8,20,35], by carbon monoxide production only. In these circumstances, CO oxidation should be catalyzed to obtain pure and reusable CO_2. However, the methods, to our knowledge, involve fine metal oxide powders (ZnO, for instance) and may induce pyrophoric effects. As an alternative, gas separation should be provided for obtaining a pure CO_2 or CO gas flux.

In an oxidant atmosphere, reactions R2c and R2d are the most likely to explain the presence of carbon dioxide;

$$CaCO_3 \leftrightarrow CaO + CO_2 \text{ (reaction R3)}$$

corresponding to the calcite to lime reaction (second decarbonation reaction).

Activation energies for the processes have been evaluated using the Coats-Redfern integral method [36–39] derived for non-reversible reactions at non-isothermal conditions (Figure S5, Supplementary Materials). The results of the analysis are reported in Table 1, along with the order of the reaction estimated on the basis of the least-square fitting agreement between the model and observations, as described by Sukarni [36]. Moreover, in CO_2 production, we classified the reaction mechanism following the method described by Dollimore [26,40]. However, our evaluation does not claim to be absolute: the Coats-Redfern approach is hardly suitable for the determination of reaction mechanisms and correct kinetic analysis of a single experimental curve requires an a priori knowledge of the true activation energy [41,42].

Table 1. Activation energies (E_{att}) and orders of the reactions (n) were evaluated by applying the Coats-Redfern method. The mechanism of reaction was hypothesized, when possible, using the approach described by Dollimore et al. [26,43].

Experimental Evidence	E_{att} (kJ/mol)	n (Best Fit)	Possible Reaction Mechanisms	Notes
1st H_2O release	241	2	not determined	The mechanism cannot be proposed due to the low value of α_{max} obtained from the Coats-Redfern method
2nd H_2O release	−22	0	not determined	The mechanism cannot be proposed due to the low value of αmax obtained from the Coats-Redfern method
CO release	118	1	not determined	The mechanism cannot be proposed due to the low value of αmax obtained from the Coats-Redfern method; Overlaps the 1st CO_2 release
1st CO_2 release	234	2	2nd order decay	Overlaps the CO release
2nd CO_2 release	51	0	1D diffusion	-

The magnitude of the activation energy values inferred here is comparable to those found in the literature [5,18,19,37]. The occurring discrepancies are attributed to the experimental setup differences in heat and mass transfer, sample particle size, and catalytic effects of the impurities present in the system.

Thermal degradation of weddellite occurs through multi-step transformations. Some overlapping of the processes occurs in water release reactions (first and second release are not fully separated), in CO_2 release reactions at low temperature, and in the combined

CO—CO_2 evolution, wherein the maximum release rates of CO and CO_2 occur at 488 and 492.6 °C, respectively. All of these overlapping processes may affect the evaluation of the activation energies of a single process. As an example, the second water release shows a negative activation energy value. This negative value is probably due to the double interference effects of first water release and CO_2 feeble release at low temperature on the second water release process. At the same time, we know that this reaction corresponds to the structural water loss, which seems unlikely to be a barrierless reaction.

A comparison of TGA results with HT-XRPD reveals a temperature shift towards higher values in the former, confirming the severe dependence of the kinetics of the reactions on the heat transfer rate and, in general, on the experimental setup.

To summarize, the feasibility of CO_2 long-term storage in crystalline oxalate stable at room temperature and pressure has been proven on microcrystalline weddellite samples from the CO_2 capture green reaction in a circular economy perspective. Even if a direct comparison of TGA and XRPD results confirms the severe dependence of the reactions' kinetics on the heat transfer rate and, in general, on the experimental setup, as expected from the literature, we demonstrated that during heating, calcium oxalate may release some CO_2 at relatively low temperature (150 °C). This must be considered the higher storage temperature for calcium oxalate to avoid the release of CO_2 back to the environment. With the exception of this faint loss of carbonate, COA guarantees that the mass of CO_2 is safely stored until the first decarbonation temperature is reached and a CO + CO_2 mixture is produced. At this step, a gas separation is required to decouple pure CO_2 from CO. Then, starting from the onset of the second decarbonation reaction (550 °C for the setup tested), pure CO_2 can be safely retrieved from COA, leaving a crystalline calcium oxide ready for further technological applications. During the pure carbon dioxide release, starting at 550 °C, the CO_2 peak rises slowly and asymmetrically due to the presence of lingering volatile species in the reaction chamber (Topley-Smith effect). The asymmetry reflects a forward-backward reaction due to the high activities of both carbon dioxide and calcium oxide substrate in the reaction chamber.

Supplementary Materials: The following are available online at https://www.mdpi.com/article/10.3390/min12010053/s1. Figure S1: Sketch of the experimental setup for CO_2 capture; Figure S2: Ramp#2 crystalline phase transitions; Figure S3: Unit cell volume (p.f.u.) of the phases formed during thermal degradation of weddellite; Figure S4: Decomposition of the FTIR curves using the Fityk free decomposition software; Figure S5: Analysis of TG data by applying the Coats-Redfern method; Table S1: Temperatures of the measurements in the HT-XRPD *in-situ* experiments (Ramp#1 to #3); Table S2: The three main steps of the decomposition reaction following Hourlier [17] summarized; Table S3: XRPD and TG summarized.

Author Contributions: Resources, M.A.; conceptualization, investigation, writing—review and editing, D.B.; conceptualization, investigation, writing—review and editing, A.C.; conceptualization, writing—review and editing, I.C.; conceptualization, investigation, formal analysis, validation, visualization, writing—review and editing, N.C.; conceptualization, investigation, formal analysis, validation, visualization, writing—original draft preparation, writing—review and editing supervision, L.P.; writing—review and editing, project administration, funding acquisition, supervision, A.P. All authors have read and agreed to the published version of the manuscript.

Funding: This research was funded by Università degli Studi di Torino (Italy), IREN S.p.A. (Italy), Ecospray S.p.A. (Italy) and Italian Ministry for Education, University and Research (MIUR; project PRIN2017-2017L83S77).

Data Availability Statement: Data are available at the following link: https://tinyurl.com/jkmna4jk (accessed on: 27 December 2021).

Acknowledgments: The authors are grateful to the anonymous referees, whose remarks, suggestions, and corrections relevantly improved the quality of the original manuscript.

Conflicts of Interest: The authors declare no conflict of interest.

References

1. Dollimore, D. The thermal decomposition of oxalates. A review. *Thermochim. Acta* **1987**, *117*, 331–363. [CrossRef]
2. Dollimore, D.; Griffiths, D.L. Differential thermal analysis study of various oxalates in oxygen and nitrogen. *J. Therm. Anal. Calorim.* **1970**, *2*, 229–250. [CrossRef]
3. Dollimore, D.; Griffiths, D.L.; Nicholson, D. The thermal decomposition of oxalates. Part II. Thermogravimetric analysis of various oxalates in air and in nitrogen. *J. Chem. Soc.* **1963**, 2617–2623. [CrossRef]
4. Kutaish, N.; Aggarwal, P.; Dollimore, D. Thermal analysis of calcium oxalate samples obtained by various preparative routes. *Thermochim. Acta* **1997**, *297*, 131–137. [CrossRef]
5. Błażejowski, J.; Zadykowicz, B. Computational prediction of the pattern of thermal gravimetry data for the thermal decomposition of calcium oxalate monohydrate. *J. Therm. Anal. Calorim.* **2013**, *113*, 1497–1503. [CrossRef]
6. Conti, C.; Brambilla, L.; Colombo, C.; Dellasega, D.; Gatta, G.D.; Realini, M.; Zerbi, G. Stability and transformation mechanism of weddellite nanocrystals studied by X-ray diffraction and infrared spectroscopy. *Phys. Chem. Chem. Phys.* **2010**, *12*, 14560–14566. [CrossRef]
7. Conti, C.; Casati, M.; Colombo, C.; Realini, M.; Brambilla, L.; Zerbi, G. Phase transformation of calcium oxalate dihydrate–monohydrate: Effects of relative humidity and new spectroscopic data. *Spectrochim. Acta Part A Mol. Biomol. Spectrosc.* **2014**, *128*, 413–419. [CrossRef]
8. Simons, E.; Newkirk, A. New studies on calcium oxalate monohydrate: A guide to the interpretation of thermogravimetric measurements. *Talanta* **1964**, *11*, 549–571. [CrossRef]
9. Pastero, L.; Curetti, N.; Ortenzi, M.A.; Schiavoni, M.; Destefanis, E.; Pavese, A. CO_2 capture and sequestration in stable Ca-oxalate, via Ca-ascorbate promoted green reaction. *Sci. Total Environ.* **2019**, *666*, 1232–1244. [CrossRef] [PubMed]
10. Pastero, L.; Marengo, A.; Boero, R.; Pavese, A. Non-conventional CO_2 sequestration via Vitamin C promoted green reaction: Yield evaluation. *J. CO2 Util.* **2021**, *44*, 101420. [CrossRef]
11. Bhattacharjee, S.; Paria, M.; Maiti, H. Preparation of $PbTiO_3$ powder through oxalate precipitation route. *Mater. Lett.* **1992**, *13*, 130–134. [CrossRef]
12. Munson, M.J.; Riman, R.E. Observed phase transformations of oxalate-derived lead monoxide powder. *J. Therm. Anal. Calorim.* **1991**, *37*, 2555–2566. [CrossRef]
13. Andrade, A.; Machado, A.J.S.; Jardim, R. Kinetic study of La_2CuO_4 formation from an oxalate precursor. *Mater. Lett.* **1992**, *13*, 96–101. [CrossRef]
14. Chen, F.-H.; Tseng, T.-Y. Formation of High-Tc Superconducting Bi-Pb-Sr-Ca-Cu Oxide Films by Spray Pyrolysis of an Oxalate Suspension. *J. Am. Ceram. Soc.* **1990**, *73*, 889–892. [CrossRef]
15. Gurrieri, S.; Siracusa, G.; Calí, R. Thermal decomposition of $CaC_2O_4 \cdot H_2O$. Determination of kinetic parameters by DTG and DTA. *J. Therm. Anal. Calorim.* **1974**, *6*, 293–298. [CrossRef]
16. Frost, R.L.; Weier, M.L. Thermal treatment of whewellite—a thermal analysis and Raman spectroscopic study. *Thermochim. Acta* **2004**, *409*, 79–85. [CrossRef]
17. Hourlier, D. Thermal decomposition of calcium oxalate: Beyond appearances. *J. Therm. Anal. Calorim.* **2018**, *136*, 2221–2229. [CrossRef]
18. Szekely, T.; Varhegyi, G.; Till, F.; Szabo, P.; Jakab, E. The effects of heat and mass transport on the results of thermal decomposition studies: Part 1. The three reactions of calcium oxalate monohydrate. *J. Anal. Appl. Pyrolysis* **1987**, *11*, 71–81. [CrossRef]
19. Price, D.; Dollimore, D.; Fatemi, N.; Whitehead, R. Mass spectrometric determination of kinetic parameters for solid state decomposition reactions. Part 1. Method; calcium oxalate decomposition. *Thermochim. Acta* **1980**, *42*, 323–332. [CrossRef]
20. Kloprogge, T.; Boström, T.E.; Weier, M.L. In situ observation of the thermal decomposition of weddelite by heating stage environmental scanning electron microscopy. *Am. Miner.* **2004**, *89*, 245–248. [CrossRef]
21. Boldyrev, V.V.; Nevyantsev, I.S.; Mikhailov, Y.N.; Khairetdinov, E.F. On the mechanism of thermal decomposition of oxalates. *Kinet. Katal.* **1970**, *11*, 367–373.
22. Kociba, K.J.; Gallagher, P.K. A study of calcium oxalate monohydrate using dynamic differential scanning calorimetry and other thermoanalytical techniques. *Thermochim. Acta* **1996**, *282–283*, 277–296. [CrossRef]
23. McAdie, H.G. Simultaneous Differential Thermal Analysis and Thermogravimetric Analysis Using the Open-Pan Type of Sample Holder. *Anal. Chem.* **1963**, *35*, 1840–1844. [CrossRef]
24. Al-Maskari, N.; McAdams, D.; Reddy, J. Modeling of a biological material nacre: Waviness stiffness model. *Mater. Sci. Eng. C* **2017**, *70*, 772–776. [CrossRef]
25. Barrall, E.M.; Rogers, L.B. Differential thermal analysis of organic samples. Effects of geometry and operating variables. *Anal. Chem.* **1962**, *34*, 1101–1106. [CrossRef]
26. Lee, Y.F.; Dollimore, D. The identification of the reaction mechanism in rising temperature kinetic studies based on the shape of the DTG curve. *Thermochim. Acta* **1998**, *323*, 75–81. [CrossRef]
27. Anderson, E.M.; Ericsson, I. Thermal degradation of organic polymers using different metals as the pyrolysis filament. *J. Anal. Appl. Pyrolysis* **1981**, *3*, 35–47. [CrossRef]
28. Windig, W.; Kistemaker, P.; Haverkamp, J.; Meuzelaar, H. The effects of sample preparation, pyrolysis and pyrolyzate transfer conditions on pyrolysis mass spectra. *J. Anal. Appl. Pyrolysis* **1979**, *1*, 39–52. [CrossRef]

29. Gál, S.; Paulik, F.; Erdey, L.; Bayer, J. Derivatographische untersuchung von calciumoxalathydraten. *Period. Polytech. Chem. Eng.* **1963**, *7*, 215–222.
30. Izatulina, A.R.; Yelnikov, V.Y. Structure, Chemistry and Crystallization Conditions of Calcium Oxalates—The Main Components of Kidney Stones. In *Minerals as Advanced Materials I.*; Springer: Berlin/Heidelberg, Germany, 2008; pp. 231–239. [CrossRef]
31. Izatulina, A.R.; Gurzhiy, V.; Krzhizhanovskaya, M.G.; Kuz'Mina, M.A.; Leoni, M.; Frank-Kamenetskaya, O.V. Hydrated Calcium Oxalates: Crystal Structures, Thermal Stability, and Phase Evolution. *Cryst. Growth Des.* **2018**, *18*, 5465–5478. [CrossRef]
32. Walter-Lévy, L.; Laniepce, J. Sur la thermolyse des hydrates de l'oxalate de calcium. *C. R. Acad. Sci. Paris* **1964**, *259*, 4686–4688.
33. Zhao, W.; Sharma, N.; Jones, F.; Raiteri, P.; Gale, J.D.; Demichelis, R. Anhydrous Calcium Oxalate Polymorphism: A Combined Computational and Synchrotron X-ray Diffraction Study. *Cryst. Growth Des.* **2016**, *16*, 5954–5965. [CrossRef]
34. Wojdyr, M. Fityk: A general-purpose peak fitting program. *J. Appl. Crystallogr.* **2010**, *43*, 1126–1128. [CrossRef]
35. Echigo, T.; Kimata, M.; Kyono, A.; Shimizu, M.; Hatta, T. Re-investigation of the crystal structure of whewellite [$Ca(C_2O_4)\cdot H_2O$] and the dehydration mechanism of caoxite [$Ca(C_2O_4)\cdot 3H_2O$]. *Mineral. Mag.* **2005**, *69*, 77–88. [CrossRef]
36. Sukarni, S.; Widiono, A.E.; Wulandari, R.; Prasetiyo, A.; Puspitasari, P. Thermogravimetric Study on the Thermal Characteristics of *Tetraselmis chuii* Microalgae Pyrolysis in the Presence of *Titanium dioxide*. *Key Eng. Mater.* **2020**, *851*, 156–163. [CrossRef]
37. Coats, A.W.; Redfern, J.P. Kinetic Parameters from Thermogravimetric Data. *Nat. Cell Biol.* **1964**, *201*, 68–69. [CrossRef]
38. Freeman, E.S.; Carroll, B. The Application of Thermoanalytical Techniques to Reaction Kinetics: The Thermogravimetric Evaluation of the Kinetics of the Decomposition of Calcium Oxalate Monohydrate. *J. Phys. Chem.* **1958**, *62*, 394–397. [CrossRef]
39. Doyle, C.D. Kinetic analysis of thermogravimetric data. *J. Appl. Polym. Sci.* **1961**, *5*, 285–292. [CrossRef]
40. Dollimore, D. The application of thermal analysis in studying the thermal decomposition of solids. *Thermochim. Acta* **1992**, *203*, 7–23. [CrossRef]
41. Ebrahimi-Kahrizsangi, R.; Abbasi, M. Evaluation of reliability of Coats-Redfern method for kinetic analysis of non-isothermal TGA. *Trans. Nonferr. Met. Soc. China* **2008**, *18*, 217–221. [CrossRef]
42. Málek, J.; Criado, J.M. Empirical kinetic models in thermal analysis. *Thermochim. Acta* **1992**, *203*, 25–30. [CrossRef]
43. Dollimore, D.; Evans, T.; Lee, Y.; Wilburn, F. Correlation between the shape of a TG/DTG curve and the form of the kinetic mechanism which is applying. *Thermochim. Acta* **1992**, *198*, 249–257. [CrossRef]